Electronic Supplementary Material (ESI) for Nanoscale.
This journal is © The Royal Society of Chemistry 2019

Supporting Information

Dynamics of Ionic Liquids in the Presence of Polymer-Grafted Nanoparticles

Siqi Liu[a], Clemens Liedel[b], Nadezda V. Tarakina[b], Naresh C. Osti[c] and Pinar Akcora*[,a]

[a]Department of Chemical Engineering & Materials Science, Stevens Institute of Technology
Hoboken, NJ 07030, USA

[b]Department of Colloid Chemistry, Max Planck Institute of Colloids and Interfaces
Research Campus Golm, Potsdam 14476, Germany

[c]Neutron Scattering Division, Oak Ridge National Laboratory
Oak Ridge, Tennessee 37831, USA

*Corresponding Author. Email: pakcora@stevens.edu

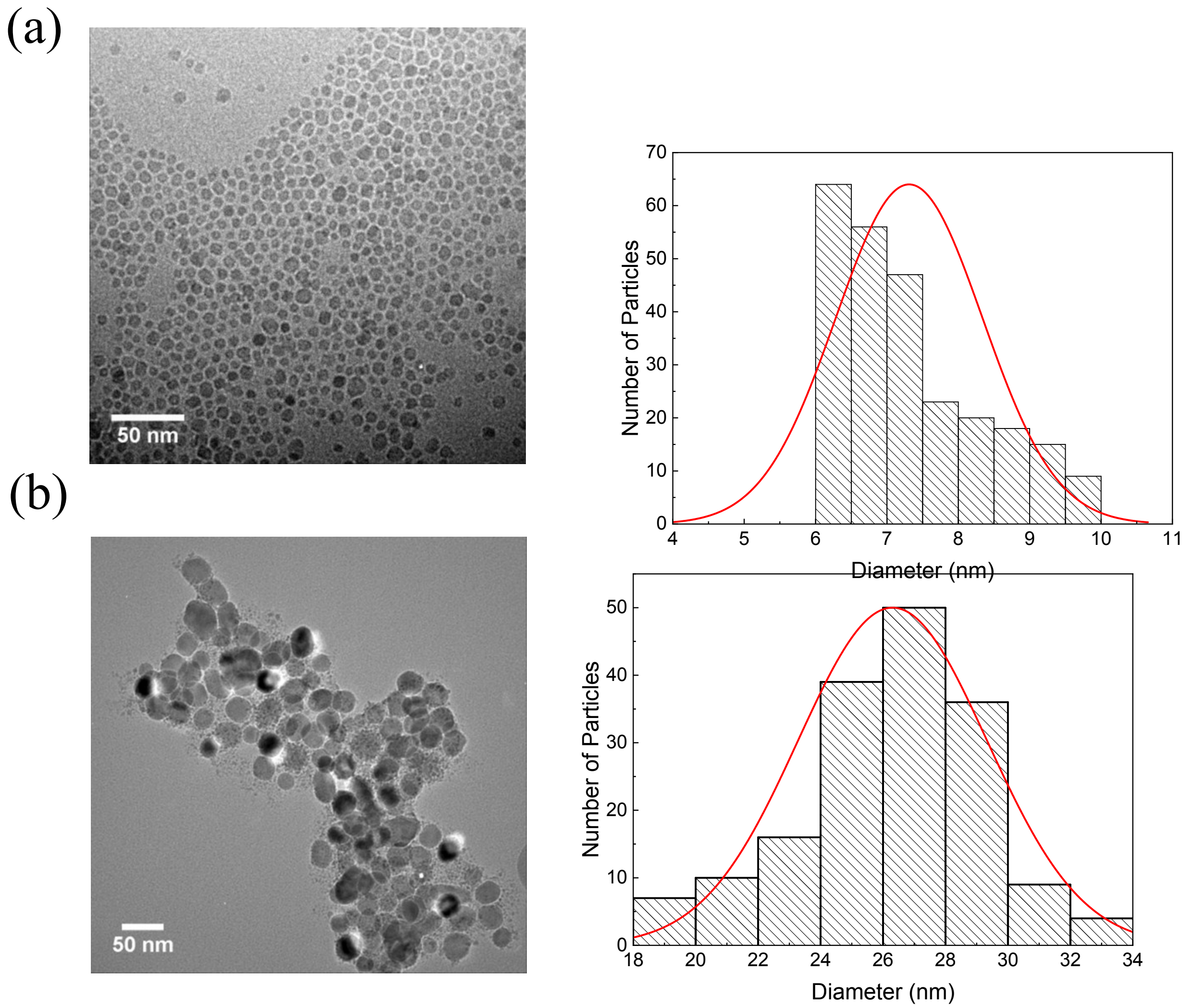

Figure S1. TEM images of **(a)** 7 nm and **(b)** 26 nm iron oxide nanoparticles and their corresponding size histograms.

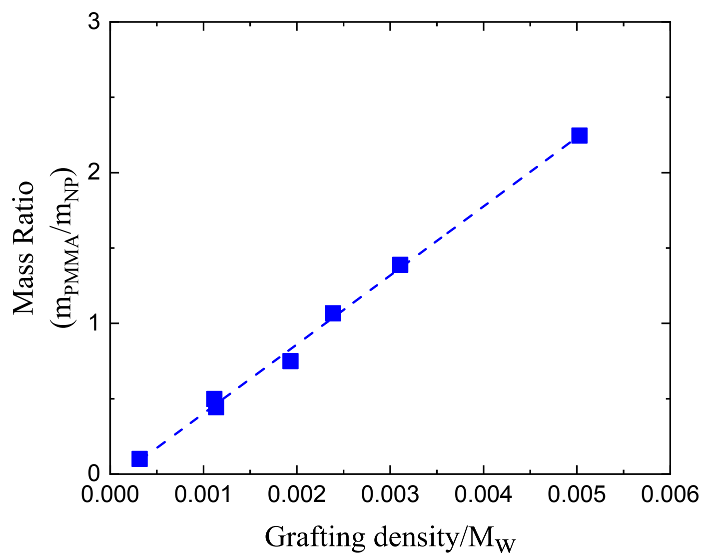

Figure S2. Mass ratio of grafted chains and core particles (m_{PMMA}/m_{NP}) as a function of the ratio of grafting density (σ) and M_w.

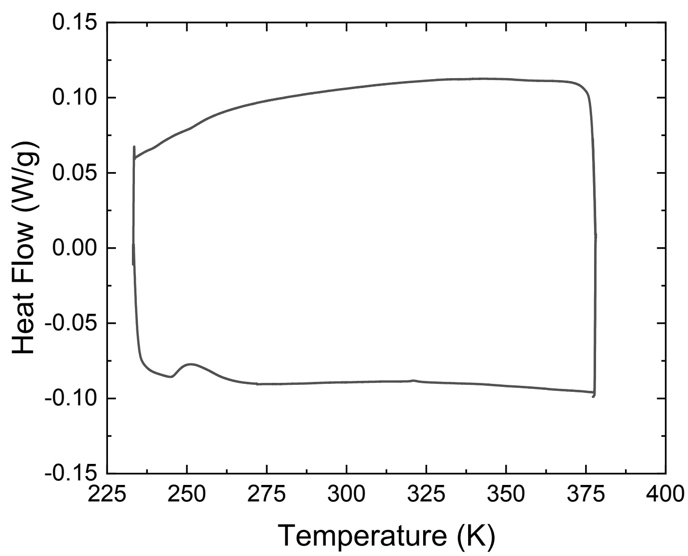

Figure S3. DSC histogram of HMIM-TFSI collected at 5K/min heating rate.

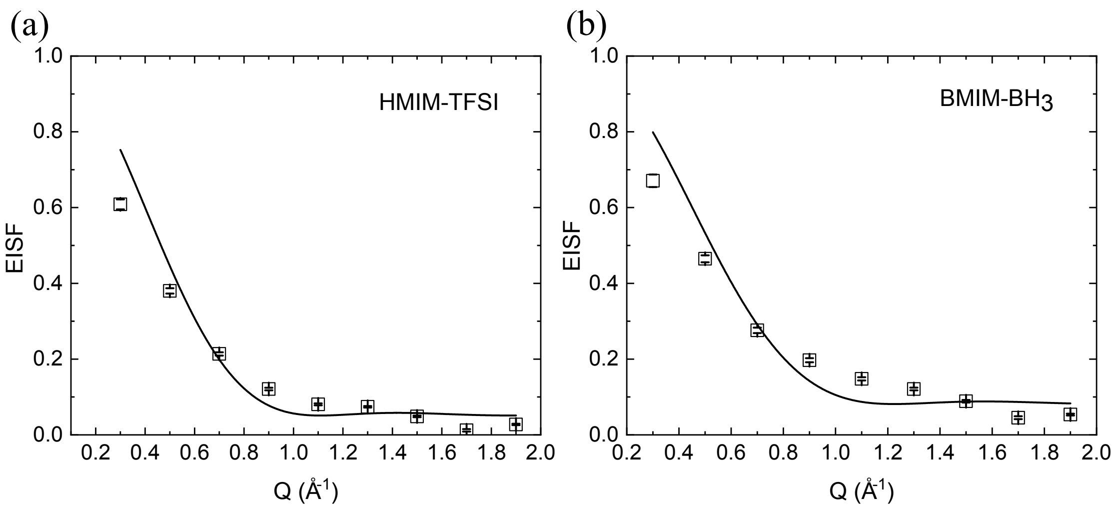

Figure S4. Elastic incoherent structure factor (EISF) of neat **(a)** HMIM-TFSI and **(b)** BMIM-BH_3 at 300 K.

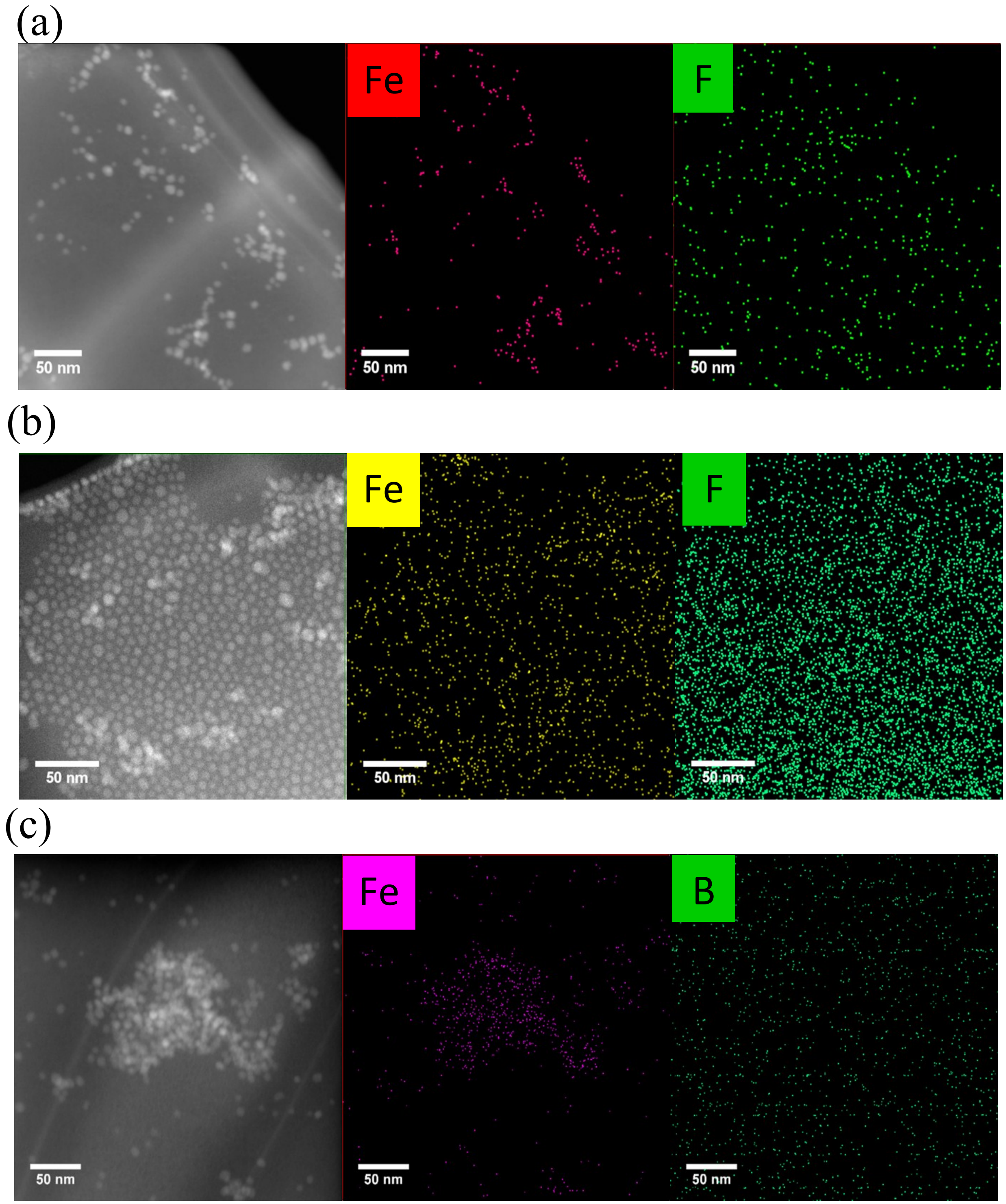

Figure S5. Dark field TEM micrographs and EDX maps of **(a)** 39.9 kDa-0.08 chains/nm^2 grafted particles in HMIM-TFSI; **(b)** 40.2 kDa-0.11 chains/nm^2 grafted particles in HMIM-TFSI; **(c)** 40.2 kDa-0.11 chains/nm^2 grafted particles in BMIM-BH_3.

Table S1. Coherent (σ_{coh}), incoherent (σ_{incoh}) and absorption (σ_{abs}) scattering cross sections of all species used in the paper.

	σ_{scatt} (cm^{-1})	σ_{coh} (cm^{-1})	σ_{incoh} (cm^{-1})	σ_{abs} (cm^{-1})
Fe_3O_4	0.694	0.64	0.054	0.359
d-PMMA	0.542	0.45	0.092	0
$C_8H_{17}BN_2$ ($BMIM-BH_3$)	5.578	0.003	5.575	10.296
$C_{12}H_{19}F_6N_3O_4S_2$ (HMIM-TFSI)	3.14	0.05	3.09	0.085
$C_{13}H_{13}NO_2S_2$ (CTA)	2.501	0.036	2.465	0.055

Table S2. Diffusion coefficients (D) of neat HMIM-TFSI and $BMIM-BH_3$; PMMA-grafted nanoparticles in HMIM-TFSI; and $BMIM-BH_3$ for **(a)** fast and **(b)** slow processes at 300 K.

(a)

	D_{fast} (10^{-10} m^2 s^{-1})			
	neat	39.9 kDa-0.08 chains/nm²	40.2 kDa-0.11 chains/nm²	138.4 kDa-0.09 chains/nm²
in HMIM-TFSI	21.46±3.99	21.40±6.14	58.04±21.67	29.53±5.15
in $BMIM-BH_3$	19.56±6.66	19.42±5.32	27.1±10.94	25.67±8.85

(b)

	D_{slow} (10^{-10} m^2 s^{-1})			
	neat	39.9 kDa-0.08 chains/nm²	40.2 kDa-0.11 chains/nm²	138.4 kDa-0.09 chains/nm²
in HMIM-TFSI	0.91±0.15	5.03±0.98	0.90±0.17	1.19±0.17
in $BMIM-BH_3$	0.76±0.13	1.08±0.20	0.88±0.15	0.87±0.11

Table S3. Characteristic residence times (τ) of neat HMIM-TFSI and BMIM-BH_3; PMMA-grafted nanoparticles in HMIM-TFSI, and BMIM-BH_3 for **(a)** fast and **(b)** slow processes.

(a)

	τ_{fast} (ps)			
	neat	39.9 kDa-0.08 chains/nm^2	40.2 kDa-0.11 chains/nm^2	138.4 kDa-0.09 chains/nm^2
in HMIM-TFSI	19.90±0.89	15.41±1.21	23.84±1.33	22.94±0.71
in BMIM-BH_3	22.95±1.82	22.75±1.47	21.08±1.69	24.48±1.57

(b)

	τ_{slow} (ps)			
	neat	39.9 kDa-0.08 chains/nm^2	40.2 kDa-0.11 chains/nm^2	138.4 kDa-0.09 chains/nm^2
in HMIM-TFSI	116.2±11.24	157.6±5.98	116.7±12.92	157.55±14.07
in BMIM-BH_3	179.4±15.89	167.3±13.49	180.4±14.27	193.98±13.49

Table S4. Jump distance $\langle l \rangle$, calculated from $D=\langle l^2 \rangle/6\tau$, of neat HMIM-TFSI and $BMIM\text{-}BH_3$; PMMA-grafted nanoparticles in HMIM-TFSI; and $BMIM\text{-}BH_3$ for **(a)** fast and **(b)** slow processes.

(a)

	l_{fast} (Å)			
	neat	39.9 kDa-0.08 chains/nm^2	40.2 kDa-0.11 chains/nm^2	138.4 kDa-0.09 chains/nm^2
in HMIM-TFSI	5.06	4.45	9.11	6.38
in $BMIM\text{-}BH_3$	5.19	5.15	5.85	6.14

(b)

	l_{slow} (Å)			
	neat	39.9 kDa-0.08 chains/nm^2	40.2 kDa-0.11 chains/nm^2	138.4 kDa-0.09 chains/nm^2
in HMIM-TFSI	2.52	6.90	2.51	3.35
in $BMIM\text{-}BH_3$	2.86	3.29	3.09	3.18